Journal of Vibration Engineering & Technologies
https://doi.org/10.1007/s42417-022-00544-6

ORIGINAL PAPER

Dynamics and Stability of Metal Cutting Circular Saws with Distributed and Lubricated Guides

Sunny Singhania[1] · **Anurag Singh**[1] · **Mohit Law**[1]

Received: 30 October 2021 / Revised: 21 March 2022 / Accepted: 23 April 2022

Abstract

Purpose This paper characterizes the dynamics and stability of metal cutting circular saws with distributed and lubricated guides. Though stability of point spring-guided circular saws is well studied, how the mass, damping, and stiffness properties of the fluid media between the rotating saw and distributed guides influences the saw's stress–stability relationship remains unexplored. Characterizing these aspects and describing how the fluid induces speed-dependent viscous shear stresses on the saw to potentially influence its cutting behaviour are the main new technical contributions of this paper.

Methods The governing equation of motion is solved using the Galerkin projection method, and through model-based investigations, we analyse the role of different lubricating fluids with differently sized guides and with changing clearances between the saw and the guides. We characterize the frequency–speed behaviour of the saw for its critical speeds and the forced vibration response of the saw using the frequency response function.

Results We note that stiffness of the fluid media plays a more significant role than its mass, damping, and/or viscosity. For large guides with stiff fluids and small clearances, instabilities occur at speeds lesser than the critical speed. For similar configurations, forced response characteristics are at least an order of magnitude dynamically stiffer than the case of the unguided saws. We further note that the free and forced vibration response for two smaller guides is better than one larger one.

Conclusions Our findings can instruct sizing and placing guides and in selecting appropriate fluid media for stabilizing metal sawing processes.

Keywords Sawing dynamics · Vibrations · Stability · Critical speed · Frequency response function

Introduction

Rotating circular saws are fed into metal bars and tubes to cut them to lengths of desired sections. To minimize kerf losses, saws are made thin. Being thin makes them flexible. They therefore tend to vibrate during free rotations, and even more so during cutting process-induced excitations. Under certain conditions, excitations, and speeds, these vibrations can grow and result in critical speed-related instabilities, regenerative instabilities, buckling instabilities, and/or flutter instabilities. To limit these instabilities, saws are usually guided.

Guides placed at some distance away from the rotating saw provide bearing surfaces to constrain the saw's lateral motion. Often, the fluid between the guide and the saw is air or water, or a mix of these [1–3]. Sometimes, during the cutting of metals, guides are lubricated with oils, or oil mists, and/or with grease. These lubricants also help reduce friction between the swarf and the saw tooth, cool the cutting region, and sometimes flush away the swarf from the cutting region. Depending on the fluid in use, lubricated guides can provide varying levels of additional stiffness, mass, and damping, and affect the viscous shear on the saw. A precise understanding of the stress–stability relationship due to the complex interactions between the spinning saw and the distributed and lubricated guides is essential to prevent unstable vibrations. Since such analysis remains unaddressed in the literature, it is the main aim of this paper to address that research gap by proposing new, expanded, and realistic models to guide stable sawing processes.

✉ Mohit Law
mlaw@iitk.ac.in

[1] Machine Tool Dynamics Laboratory, Department of Mechanical Engineering, Indian Institute of Technology Kanpur, Kanpur 208016, India

Published online: 16 May 2022

The stability problem of spinning discs constrained by stationary load systems is common to circular sawing processes, to disc drives, and to brakes and clutches. The problem is hence well studied and understood [4–9]. The allied problem of a stationary disc with concentrated rotating loads has also been studied [10–15]. In the context of guided circular sawing, modelling the interaction between the saw and lubricated guide is not trivial, and hence the stationary load systems, i.e. the guides are usually modelled as spatially fixed linear elastic springs [2, 6, 16–18], and sometimes as spring–mass–damping systems [19, 20]. Introduction of multiple guides modelled as point springs has been reported to increase critical speeds more than a single guide. Damping is reported to play a stabilizing role below the critical speed, and potentially cause instabilities at speeds higher than the critical speeds. Mass appears to play no role. Though guides are recommended to be placed near the cutting zones, the optimum number, location, and relative flexibilities of such guides influencing saw stability is a matter ongoing study. Moreover, existing theories for saws with stationary loads modelled as spring–mass–damping systems requires some extension to cover the case of the lubricating fluid potentially influencing the state of stress in the saw. Characterizing this behaviour is our modest new technical contribution to the state of the art.

Since the fluid media can potentially affect the stress state in the saw, its influence can be thought akin to those devices and applications in which the stationary load also influences the saw's stress state such as in disk drives, and in brakes and clutches. In those applications, since the load is always in contact, friction at the interface loads the spinning discs in circumferential shear and tends to destabilize certain vibration modes over the entire rotational speed range [8, 12, 21–23]. Moreover, heat generation at the interface due to friction may change the dynamics and stability of the disk [24]. In metal sawing, however, there is always a finite amount of clearance between the rotating saw and the fixed guide. Moreover, since there is a fluid in the clearance, heat generation at the interface may also not be as important as it is applications in which the load is always in contact. Hence, findings from allied fields of disk drives, brakes, and clutches are not directly relevant for our investigations.

Since circular sawing of metals is almost always conducted in the presence of distributed and lubricated guides, and even though the fluid may influence circumferential shear in the saw and destabilize it like in the case of disc drives, and brakes and clutches, industrial praxis does not report saws always becoming unstable in the presence of lubricated guides. This discrepancy between theory and practice is likely due to the inadequate theoretical model for circular sawing with distributed and lubricated guides. Though there have been attempts at modelling the influence of viscous fluids between rotating discs and stationary constraints [25, 26], those studies did not investigate how the fluid influences the state of stress in the saw, and hence are not appropriate for our application of interest. Hence, an effort is made herein to make a more accurate model that accounts for how the viscous shear caused by the fluid is also a function of the saw's rotation speed.

The intention of this paper is to describe the features of a saw with lubricated guides that control its cutting behaviour. Since metals are cut at speeds typically lower than critical, and since critical speed instability is generally reached before the buckling instability condition [27] and/or the flutter instability condition [28, 29], we limit our analysis in this paper to the sub-critical and critical regimes. Since saws experience forced excitation during cutting, we also analyse forced vibration response at typical cutting regimes. Though cutting forces can result in regenerative instabilities, those are presently ignored. Moreover, though the saw has multiple teeth, and even though their geometry may influence the forced vibration response, in this paper, attention will be confined to the dynamics of the saw subject to forces distributed over a sector that is in contact with the workpiece, and the influence of teeth geometry will be ignored. We also ignore the role of the properties of the metal being cut and focus only on the saw's dynamics. We also focus herein only on saws made of standard steels and ignore the role of dynamics influenced by saws made of materials with high specific strengths [30].

Since the saw's geometry, its boundary conditions, its initial stress state, its speed of rotation, the size and the number of guide pads being used, the lubricant media between the saw and the guide, and the distance of guide pad(s) from the saw may each govern the dynamics of the system, and since the experimental try-and-see approach is prohibitive and expensive and experiments to test for critical speeds and other instability mechanisms can be destructive and damage parts of the equipment, this paper will adopt model-based investigations that will incorporate all major influences on the saw vibrational response to help instruct the design of stable sawing processes. Model-based investigations presented herein are expected to help inform experiments in future works.

Since the dynamics of spinning discs is an important technological problem, the literature on the subject is vast and varied, and it is not our aim to critically review the many seminal contributions made over the past century. However, to contextualize the main differentiating aspects of our work from other prior work, we draw attention to:

1. how our inclusion of the lubricating fluid affecting the saw's stress state and how the stress state also depends on the saw's speed is different fromn previous reports [8] in which the shear stress was assumed constant, and as such our treatment is more realistic,

2. how our modelling of the guide(s) being distributed is different from other reports [2, 6, 16–20] and is also more realistic,
3. how our modelling of the mass, damping, and stiffness properties of the fluid being a function of the guide size and its placement relative to the saw is realistic, and is different from earlier reports [2, 6, 16–20],
4. how our modelling treatment facilitates easy analysis for changing lubricating media along with changing size of guide(s), multiple guides, and distance of guide(s) from the rotating saw, and,
5. how our analysis allows for evaluation of forced vibration response for defined engagements of the saw with a bar using frequency response functions to characterize the dynamics.

The remainder of the paper is organized as follows. At first, in the second section, we describe the governing equations of motion with distributed and lubricated guides. These equations include stresses due to rotation as well as stresses generated due to viscous shear on account of the fluid media. The models follow prior reported work [6, 8]. We solve these equations to obtain the saw's free and forced vibration response, and to obtain the frequency–speed characteristics of the guided saws. The third section then discusses and analyses results with changing fluid media, changing size of guides, different number of guides as well as changing distance between the saw and the guide(s). The fourth and final discusses the significance of our investigations and lists the main conclusions.

Model of a Rotating Saw with Distributed and Lubricated Guides

We consider a guided saw rotating with an angular velocity of Ω in the counterclockwise direction. The saw is cutting a bar. The instantaneous engagements with the bar are characterized by an entry angle, γ_{st}, and an exit angle, γ_{ex}. See Fig. 1. For representation, Fig. 1 only shows a single-guide pair. These guides are placed circumferentially between γ_1 and γ_2 with their inner and outer radii being r_1 and r_2, respectively. The guides are assumed fixed and placed some distance away from the surface of the saw. The fluid between the saw and the guides offers a bearing surface with distributed stiffness, mass, and damping. The fluid also influences the saw's stress state.

Since the saw is thin, we use the von Kármán plate theory to develop an analytical model. We hence ignore the effect of transverse shear deformation and assume that the normal to the undeformed middle plane remains straight and normal to the deformed middle plane of the saw. We ignore any in-plane buckling. In addition, we assume that:

1. the saw's initial state is stress free, i.e. tensioning by cold rolling and/or forging is ignored, as is any potential thermal tensioning,
2. the saw is rigidly clamped at $r = b$, and free at its periphery at $r = a$, i.e. the collar is not floating as it sometimes is in the wood cutting application, but fixed—since that is how it is in metal cutting, and thus there is no tilting and/or rigid body motion of the saw,
3. the saw is made of viscoelastic material with an internal damping force proportional to the strain rate,
4. the saw is flat and that there is no static deflection,
5. the fluid is Newtonian and incompressible,

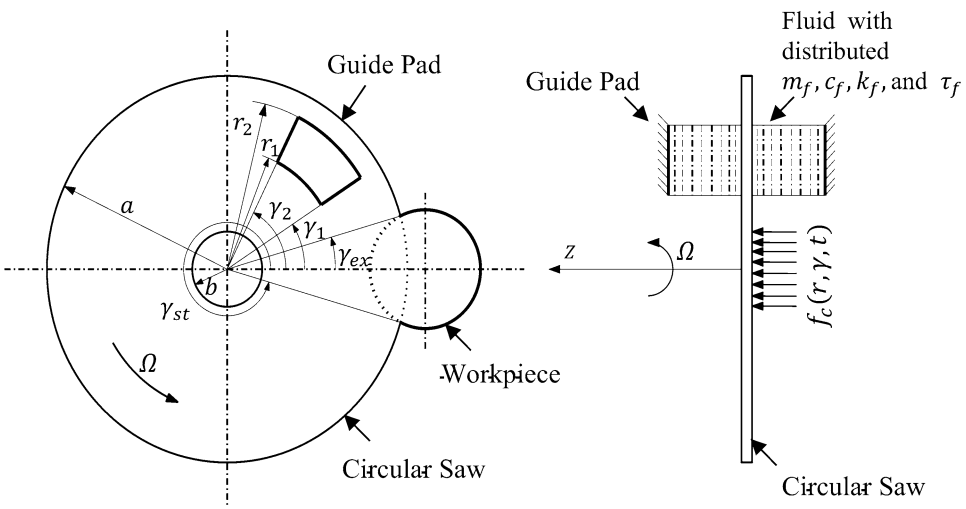

Fig. 1 Schematic representation of a circular saw with distributed and lubricated guides cutting a bar

6. the saw vibration is small and much smaller than the fluid film thickness, and the pressure variations across the fluid film thickness are negligible,
7. mass, stiffness, and damping of the fluid are a function of the fluid properties, the size of the guide and the distance between the guide and the saw, and that these do not change with speed and are uniform across the guide,
8. the viscous shear is a function of the viscosity of the fluid and the distance between the guide and the saw, and that it is proportional to the tangential speed of the saw, and this too is uniform across the guide,
9. the two guides on either side of the saw are identical, and as such, the effective distributed mass, stiffness, damping, and viscous shear intensity is twice that of a single guide.

Based on these assumptions, the governing differential equation of a rotating saw for its transverse vibration, $\tilde{w}$, in the space fixed coordinate system (r, γ, t) from its rotating coordinate system (r, θ, t) with a transformation of $w(r, \theta, t) = w(r, \gamma - \Omega t, t) = \tilde{w}(r, \gamma, t)$, and under a sector of distributed mass, stiffness, damping, and viscous shear intensity can be derived by use of the extended Hamilton's principle, which on simplification using the variational method becomes [31]

$$D\nabla^4\tilde{w} + D^*\nabla^4(\tilde{w}_{,t} + \Omega\tilde{w}_{,\gamma}) + \rho h\{\tilde{w}_{,tt} + 2\Omega\tilde{w}_{,t\gamma} + \Omega^2\tilde{w}_{,\gamma\gamma}\} - \frac{h}{r}\left\{(r\sigma_r\tilde{w}_{,r} + \sigma_{r\gamma}\tilde{w}_{,\gamma})_{,r} + \left(\frac{\sigma_\gamma}{r}\tilde{w}_{,\gamma} + \sigma_{r\gamma}\tilde{w}_{,r}\right)_{,\gamma}\right\} = f(r, \gamma, t), \tag{1}$$

wherein the comma-subscript notation signifies partial differentiation, ρ is the mass density, and h is the saw's thickness. $D = \frac{Eh^3}{12(1-\nu^2)}$ is the flexural rigidity, wherein E is the Young's modulus and ν is the Poisson's ratio. $D^* = \eta D$ is the internal damping in the saw, wherein η is the Kelvin–Voigt damping parameter, ∇^4 is the bi-harmonic operator, and σ_r, σ_γ and $\sigma_{r\gamma}$ are the in-plane stresses due to rotation and viscous shear on account of the fluid media. $f(r, \gamma, t)$ in Eq. (1) is the uniformly distributed force on the saw that comprises forces due to the distributed and lubricated guides, $f_g(r, \gamma, t)$, and the lateral forces due to cutting, $f_c(r, \gamma, t)$. These forces take the form of:

$$f_g(r, \gamma, t) = \sum_{j=1}^{J}\left[\left\{-m_{f_j}\tilde{w}_{,tt} - c_{f_j}\tilde{w}_{,t} - k_{f_j}\tilde{w}(r, \gamma, t)\right\}\left\{H\left(\gamma - \gamma_{1_j}\right) - H\left(\gamma - \gamma_{2_j}\right)\right\}\left\{H\left(r - r_{1_j}\right) - H\left(r - r_{2_j}\right)\right\} + \tau_{fj}\left(\frac{1}{r}\tilde{w}_{,\gamma}\right)\right] \tag{2}$$

and

$$f_c(r, \gamma, t) = P(r, \gamma, t)\left[H\left(r - r_1\right) - H\left(r - r_2\right)\right]\left[H\left(\gamma - \gamma_{ex}\right) - H\left(\gamma - \gamma_{st}\right)\right],$$

wherein $m_{f_j}, c_{f_j}, k_{f_j}, \tau_{fj}$ are the uniformly distributed mass, damping, stiffness, and the viscous shear stress of the fluid media between the jth guide pad pair and the saw, respectively. J in Eq. (2) is the total number of guide pad pairs, $P(r, \gamma, t)$ is the lateral force acting over the sector of the saw in contact with the bar, and $H(.)$ is the Heaviside function.

To simplify the complex interaction at the interface between the saw and the guide, we model the uniformly distributed mass, stiffness, and damping of the fluid as: $m_f = \rho_f h_f, k_f = \frac{E_f}{h_f}$, $c_f = 2\zeta\sqrt{k_f m_f}$, respectively, wherein ρ_f is the density of the fluid media, E_f is its stiffness constant, ζ is damping ratio of the fluid, μ_f is its viscosity, and h_f is clearance between the guide and saw. Assuming shear stress distributed in a sector, the viscous shear stress between the jth guide pad pair and the saw, τ_{fj} can be written in the Fourier expansion form as:

$$\tau_{fj} = \left(\tau_0 + \sum_{k=1}^{K}\tau_k\cos(k\gamma)\right)F(r), \tag{3}$$

wherein $\tau_0 = \left(\frac{\gamma_{2j} - \gamma_{1j}}{2\pi}\right)\tau$, in which $\tau = \mu_f \times \frac{V_s}{h_f}$ with V_s being the average tangential speed of the saw in the guided region. Our choice of the form for τ_{fj} makes it depend on the saw's geometry, its speed, the clearance between it and the guide, and the nature of the fluid between them. Consequently, the dynamics and stability of the rotating saw change with the lubrication medium, clearance, and guide size.

τ_k in Eq. (3) is a harmonic function, such that $\tau_k = \frac{2\tau\left(\sin\frac{k\left(\gamma_{2j} - \gamma_{1j}\right)}{2}\right)}{k\pi}$, with $k = 1, 2, \ldots K$ being the assumed number of terms in the Fourier expansion. $F(r)$ in Eq. (3) is a piecewise radial distribution function with $\mathbb{C}^1$ continuity that is chosen to work in conjunction with the Heaviside function to avoid discontinuities in generated stresses.

The model presented in Eqs. (1)–(3) accounts for the distributed guide–-fluid–saw interaction with the fluid's mass, stiffness, and damping properties modelled as a function of the guide size and its placement relative to the saw. The model also accounts for viscous shear stress on the saw changing with saw speed, and as such, the model differs from

most earlier reports in which the guided circular saw interaction was modelled only as a point spring [2, 6, 16–20].

The boundary conditions for the saw being clamped at its centre and free at its periphery are:

$$\tilde{w}(b,\gamma,t) = \tilde{w}_{,r}(b,\gamma,t) = 0, M_{rr}(a,\gamma,t) = Q_r(a,\gamma,t) - \left(\frac{1}{a}\right)\frac{\partial}{\partial\gamma}\left(M_{r\gamma}(a,\gamma,t)\right) = 0, \tag{4}$$

wherein $M_{rr}, M_{r\gamma}$ are bending moments and Q_r is shear force. The in-plane stresses induced by rotation and the viscous shear stress are superposed to obtain the total in-plane stresses. The stresses due to rotation σ_{rr} and $\sigma_{\gamma r}$ can be determined by solving the following equations [6]:

$$\sigma_{rr,r} + \frac{1}{r}\left(\sigma_{rr} - \sigma_{\gamma r}\right) + \rho r\Omega^2 = 0, \epsilon_{\gamma_r} - \epsilon_{rr} + r\frac{d\epsilon_{\gamma r}}{dr} = 0, \tag{5}$$

wherein ϵ_{rr} and ϵ_{γ_r} are the in-plane radial and circumferential strains. For the saw being clamped at its inner radius (i.e. $r = b$) and free at its periphery, the solutions to Eq. (5) are:

$$\sigma_{rr} = \left(\frac{1}{8}\right)\rho\Omega^2 a^2\left(A_1 + A_2 - A_3\right),$$

$$\sigma_{\gamma r} = \left(\frac{1}{8}\right)\rho\Omega^2 a^2\left(A_1 - A_2 - A_4\right), \tag{6}$$

wherein $A_1 = \frac{\left[(1+\nu)(3+\nu)+\left(1-\nu^2\right)\left(b'\right)^4\right]}{\left[(1+\nu)+(1-\nu)\left(b'\right)^2\right]}$, $A_2 = \frac{\left[\frac{\left(b'\right)^2}{\left(r'\right)^2}\right]\left[(1-\nu)(3+\nu)-\left(1-\nu^2\right)\left(b'\right)^2\right]}{\left[(1+\nu)+(1-\nu)\left(b'\right)^2\right]}$, $A_3 = (3+\nu)\left(r'\right)^2$ and $A_4 = (1+3\nu)\left(r'\right)^2$ with the ratio of radii being $b' = \frac{b}{a}$, and the non-dimensional radial co-ordinate being $r' = \frac{r}{a}$. These in-plane stresses due to rotation are a function of the speed of the saw and of the saw's geometry. Though our models were built on Ref. [6], it differs from it in our treatment of the distributed nature of lubricated guides affecting the stress state of the saw.

The viscous shear stress induced on the disc on account of the fluid is directed tangent to the saw's lateral motion. For small motion, the in-plane membrane stresses and displacements can be assumed to decouple from $\tilde{w}$, so that the thin plate treatment remains valid. Our treatment for viscous shear follows the model in earlier reported work [8]. The non-dimensional force balance along the radial and tangential directions with zero radial forces, and with the non-dimensional viscous shear stress τ in the angular direction can be shown to be:

$$\left(\sigma^*_{r_f}\right)_{,r'} + \frac{1}{r'}\left(\sigma^*_{r\gamma_f}\right)_{,\gamma} + \frac{1}{r'}\left(\sigma^*_{r_f} - \sigma^*_{\gamma_f}\right), = 0$$

$$\frac{1}{r'}\left(\sigma^*_{\gamma_f}\right)_{,\gamma} + \left(\sigma^*_{r\gamma_f}\right)_{,r'} + \frac{2}{r'}\sigma^*_{r\gamma_f} + \tau^* = 0, \tag{7}$$

wherein $\tau^* = \tau_f * \left(\frac{a^3}{D}\right) = \left(\frac{a^3}{D}\right)\left(\tau_0 + \sum_{k=1}^{K}\tau_k\cos(k\gamma)\right)F(r')$ is the non-dimensional viscous shear stress with $r' = \frac{r}{a}$, and $\sigma^*_{r_f}, \sigma^*_{\gamma_f}, \sigma^*_{r\gamma_f}$ are the non-dimensional in-plane stresses generated due to viscous shear in radial, tangential, and shear directions, respectively. Though our model builds on prior work [8], it differs from that by assuming that τ_f changes with the saw's speed.

Using stress–strain and the strain–displacement relationships, the non-dimensional stresses can be expressed in terms of non-dimensional radial (u') and circumferential (v') displacements through:

$$\begin{aligned}
\sigma^*_{r_f} &= 12\left(\frac{a}{h}\right)^2\left(u'_{,r'} + \nu\frac{u'}{r'} + \nu\frac{v'_{,\gamma}}{r'}\right)\\
\sigma^*_{\gamma_f} &= 12\left(\frac{a}{h}\right)^2\left(\nu u'_{,r'} + \frac{u'}{r'} + \frac{v'_{,\gamma}}{r'}\right)\\
\sigma^*_{r\gamma_f} &= 6(1-\nu)\left(\frac{a}{h}\right)^2\left(\frac{1}{r'}u'_{,\gamma} + v'_{,r'} - \frac{v'}{r'}\right).
\end{aligned} \tag{8}$$

On substituting Eq. (8) in Eq. (7), we get coupled partial differential equations in terms of in-plane displacement and non-dimensional viscous shear stress that can be written as:

$$2u'_{,r'r'} + \frac{2}{r'}u'_{,r'} - \frac{2u'}{(r')^2} + \frac{1-\nu}{(r')^2}v'_{,r'\gamma} - \frac{3-\nu}{(r')^2}v'_{,\gamma} = 0,$$

$$\frac{3-\nu}{(r')^2}u'_{,\gamma} + \frac{1+\nu}{r'}u'_{,r'\gamma} + (1-\nu)v'_{,r'r'} + \frac{1-\nu}{r}v'_{,r'} + \frac{2}{(r')^2}v'_{,\gamma\gamma} - \frac{1-\nu}{(r')^2}v' + \frac{1}{6}\left(\frac{h}{a}\right)^2\tau^* = 0. \tag{9}$$

Solutions for displacements and stresses are obtained by considering the symmetry and orthogonality condition in γ, and by assuming the displacements u' and v' to be represented in Fourier series as:

$$u' = \sum_{k=1}^{K} p_k\left(r'\right)\sin(k\gamma),$$

$$v' = q_0\left(r'\right) + \sum_{k=1}^{K} q_k\left(r'\right)\cos\left(k\gamma\right). \tag{10}$$

On substituting τ^*, u' and v' using Eqs. (3) and (10) in Eq. (9), we get residue expressions in terms of Fourier coefficients, $p_k(r')$ and $q_k\left(r'\right)$. As the solutions to Eq. (9) are assumed in the form of harmonic approximations, the method of harmonic balance is applied to approximate the

periodic solutions [32]. Suitable choice of expansion terms and the use of the harmonic balance method results in coupled differential equations in terms of the Fourier coefficients. These coefficients are obtained from the solutions to the differential equations by using the state space and the integration factor methods. These non-dimensional membrane stresses are converted to the dimensional form by multiplying with $\frac{D}{ha^2}$.

The in-plane stresses due to viscous shear together with the in-plane stresses due to rotation are used in solving the governing equation of motion. An approximate solution of the governing equation is obtained using an assumed solution of the form of [6]:

$$\tilde{w}(r,\gamma,t) = \sum_{m=0}^{M}\sum_{n=0}^{N}[\cos(n\gamma)\ \sin(n\gamma)]\{\mathrm{x(t)}\}R_{mn}(r), \tag{11}$$

wherein M and N represent the number of nodal circles and nodal diameters, respectively, and $\{x(t)\}$ is an array of $\left\{C_{mn}(t)S_{mn}(t)\right\}^T$, wherein $C_{mn}(t)$ and $S_{mn}(t)$ are the coefficients to be determined by substituting $\tilde{w}(r,\gamma,t)$ in the governing equation and applying the Galerkin procedure. $R_{mn}(r)$ is a radial shape function and is taken to be in the form of a polynomial in r as:

$$R_{mn}(r) = E^0_{mn}r^m + E^1_{mn}r^{m+1} + E^2_{mn}r^{m+2} + E^3_{mn}r^{m+3} + E^4_{mn}r^{m+4}, \tag{12}$$

wherein E^p_{mn} with $p = 0, 1, \ldots, 4$ are unknowns to be determined from the boundary conditions and displacement normalization condition.

Substituting the assumed solution in the governing equation of motion and naming the residue as $L(\tilde{w})$ and applying the Galerkin's procedure, we get:

$$\int_0^{2\pi}\int_b^a L(\tilde{w})\left[R_{ql}(r)\cos(l\gamma)\right]r\mathrm{d}r\mathrm{d}\gamma = 0,$$

$$\int_0^{2\pi}\int_b^a L(\tilde{w})\left[R_{ql}(r)\sin(l\gamma)\right]r\mathrm{d}r\mathrm{d}\gamma = 0, \tag{13}$$

wherein $l = 0, 1, 2, \ldots, M$, and $q = 0, 1, 2, \ldots, N$.

Equation (13) results in a set of coupled differential equations, which on simplification and re-arranging in a matrix form become:

$$[A]\{\ddot{x}(t)\} + [B]\{\dot{x}(t)\} + [C]\{x(t)\} = \{F(t)\}, \tag{14}$$

wherein $[A]$, $[B]$, and $[C]$ represent the mass, gyroscopic, and stiffness matrices, respectively, and $\{F(t)\}$ is the external forcing vector. We solve this equation for the free and forced vibration response of the guided saw.

For the case of the free vibration response, we assume a solution of the form of $\{x(t)\} = \{X\}\mathrm{e}^{\lambda t}$, wherein λ is a complex number whose imaginary part corresponds to the natural frequency of the system and the real part corresponds to the growth and/or decay. The response of the system is obtained on substituting $\{x(t)\}$ in the assumed form of solution, i.e. in Eq. (11). To get a sense of the frequency–speed characteristics of the guided rotating saw, Eq. (14) is solved for every speed of interest for the different configurations of fluid media, and different number, location(s), and size of guide pad(s).

For the case of the forced vibration response, we assume that the lateral component of the periodic cutting force (F_c) that excites the saw is harmonic with an excitation frequency of ω_f. The complex coefficient array to such excitations is also harmonic, and becomes:

$$\{x(t)\} = \left[\left([C] - [A]{\omega_f}^2\right) + i[B]\omega_f\right]^{-1}\left\{F_c\right\}e^{i\omega_f t}. \tag{15}$$

The real part of the complex coefficient array when substituted in Eq. (11) results in the transverse displacement of the saw for defined excitation. As with the case of the free vibration response, the forced vibration response can be evaluated for different configurations of fluid media, and different number, location(s), and size of the guide pad(s) under defined loading scenarios. Since the steady state forced vibration response is independent of any initial conditions, such analysis is useful. However, a comprehensive overview for how the saw might respond to different excitations is provided through evaluation of frequency response functions (FRFs) which characterize the response of the saw for defined inputs as a function of excitation frequency. For the range of excitation frequencies of interest, the FRF is obtained by substituting the real part of the complex coefficient array obtained from Eq. (15) in the assumed form of the solution, i.e. in Eq. (11), for assumed unit forcing. As in the case of the free and forced response analysis, the FRF is also evaluated for different configurations of fluid media, and number, location, and size of guide pads.

The proposed model, albeit in simpler forms, has already been verified [20, 33, 34] by benchmarking frequency–speed characteristics and critical speed results with earlier work [6, 35] for the case of a guide modelled only as a point spring, and by separately benchmarking stress fields with other reported work [8] for the for the case of a guide (brake) always in contact with a rotating disc. Since the model is deemed verified, and since the dynamics and stability of circular sawing of metals with distributed and lubricated guides is more nuanced than previous models can characterize, systematic model-based investigations are presented next.

Numerical Analysis of Circular Saw with Distributed and Lubricated Guides

All analysis presented herein is for a representative saw made of steel with a density of 7850 kg/m^3, a modulus of 210 GPa, and with a Poisson ratio of 0.3. The saw's

clamped diameter is 85 mm. Its outer diameter is 285 mm, and its thickness is 2 mm. The saw's internal damping characterized by the Kelvin–Voigt damping parameter η is taken to be 10^{-6} s. The saw is assumed to be cutting a bar with a diameter of 76 mm. For the case of the forced response analysis, the saw is assumed to have 60 teeth, and its instantaneous engagement with the bar is assumed to have an entry angle of $\gamma_{st} = 344^0$, and an exit angle of $\gamma_{ex} = 16^0$, measured counterclockwise.

Since saw vibration modes that dominate transverse motion consist of one to four nodal diameters and zero nodal circles [16], all analysis herein will be limited to this multi-mode configuration. Furthermore, for all analysis herein, the guide, when present, is assumed to be placed between a radial location of $r_1 = 0.7a$ and $r_2 = 0.9a$. This location is chosen such that the saw may be able to completely part the bar being cut. The circumferential location of the single and/or multiple guides is varied to understand its influence on the saw's dynamics and stability. The clearance between the guide(s) and the saw is similarly varied to understand its role. Together with changing the size of the guide and the clearance between the saw and the guide, the role of three different lubricating media, namely, air, oil, and grease is also investigated. The mass density ρ_f, stiffness constant E_f, and the viscosity μ_f of the fluid media are taken as listed in Table 1. The damping ratio for all fluids is assumed to be $\zeta = 0.001$, and because of the stiffness and mass of the fluids being different, the damping coefficient for different fluids is also different, with oil offering more damping than air, and grease more than oil.

In the following sub-sections we present the free and forced response of the guided saw with different configurations of fluid media, and number, location, and size of guide pads.

Lubricated Single Guide

At first, we present the response of an oil-lubricated guided saw and contrast its response with a saw that is not guided. We follow that analysis with the response of the saw with differently lubricated guides. Those discussions are followed by how for an oil-lubricated guide, the size of the guide and the clearance between the saw and the guide influences response.

Table 1 Properties of the lubricant fluid medium [3, 36]

Lubricant	Stiffness constant E_f (Nm^{-2})	Viscosity μ_f (Pa s)	Mass density ρ_f (kgm^{-3})
Air	45	1.8×10^{-5}	1.12
Oil	45×10^3	17.6×10^{-3}	800
Grease	65×10^3	0.1	900

Oil-Lubricated Guide

The guide is placed between $\gamma_1 = 22^0$ and $\gamma_2 = 52^0$, i.e. close to the cutting zone as recommended [2]. The clearance between the saw and the guide is taken to be 0.15 mm, which is typical of metal cutting operations. To get a sense of how the fluid's mass, stiffness, damping, and viscous shear, each influence the dynamics and stability of the saw, response for each case was obtained separately. For the free vibration case, the real and imaginary parts of the eigenvalues were evaluated to characterize the frequency–speed characteristics for each configuration. These are shown in Fig. 2.

As is evident from Fig. 2, the response of a guided saw is significantly different from a saw without one. From Fig. 2a, which shows the imaginary part of the eigenvalue changing with speed, it is evident that the frequency of the so-called backward travelling wave is decreased by rotation, while that of the forward travelling wave is increased. The real parts of the eigenvalues at these critical speeds are positive—as is evident from Fig. 2b, suggesting that the response will grow with the slightest perturbations at these speeds. At all speeds below critical, the real parts of the eigenvalues are zero and/or negative.

The frequency–speed characteristics for a guided saw being different from one that is not guided is also evident from Fig. 2a. The first mode to become critical in the guided case is the 0.1 mode, whereas for the case without a guide it is the 0.3 mode. These differences are consistent with other reported behaviour [6]. Figure 2a also suggests that even with the fluid modelled as only a spring, the critical speed increases marginally in comparison to a saw that is not guided. This increase, even if slight, is likely due to the guide being modelled as distributed, and hence is different fromn the case of the guide being modelled as a point spring—in which the critical speed is reported to not increase [2, 6, 20].

The influence of mass, damping, and viscous shear due to the oil-lubricated guides is also evident from response comparisons in Fig. 2. The mass and damping of the fluid appear to play no role in the frequency–speed characteristics in the sub-critical speed regions. However, damping increases the rate of growth of response at super-critical speeds —see Fig. 2b. These observations are consistent with other earlier reported findings [4, 11]. For this oil-lubricated guide, even though the fluid changes the stress state of the saw, the fluid's viscosity does not change the critical speed, and/or the sub- and super-critical regimes. This observation is consistent with industrial praxis for

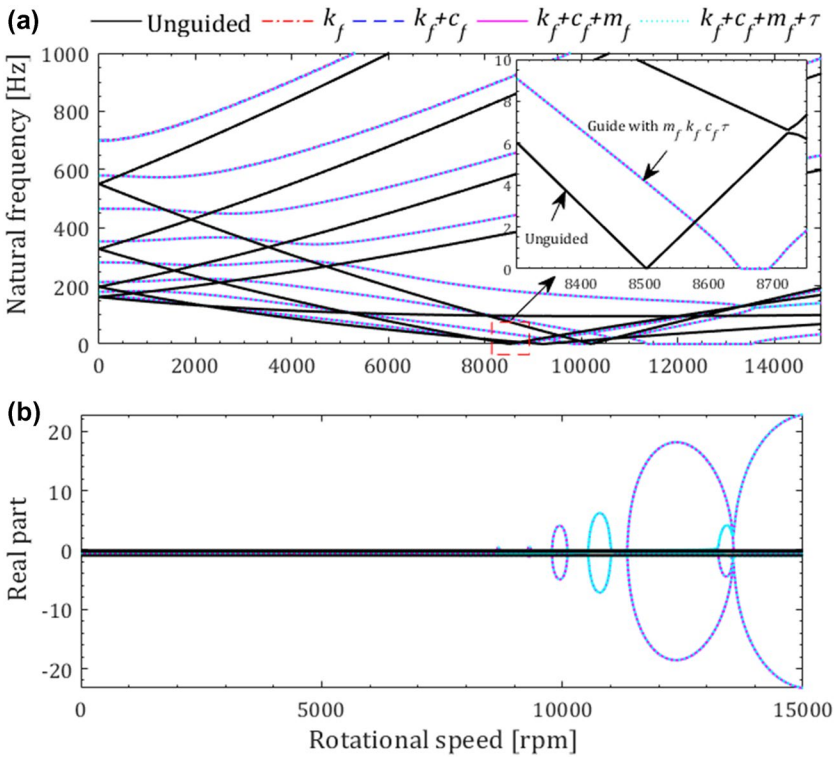

Fig. 2 Comparison of speed characteristics for an oil-lubricated guided saw with and without a guide. **a** Frequency–speed characteristics, **b** real part of the eigenvalue changing with speed

metal sawing processes and is different fromn other reports in which frictional constraints in contact with rotating discs always destabilize systems.

Since steels are cut at speeds typically significantly lower than the critical, and within the cutting speed range of 100–250 m/min [37], the forced response is also of interest. This forced response, evaluated at the outer edge of the middle of the sector in contact with the workpiece, i.e. at $\gamma = 0^{o}$, is characterized through the FRFs shown in Fig. 3. For the cutting speed range of interest, the corresponding rotational speed range of interest becomes ~ 90 to ~ 225 rotations per minute (cutting speed $= \pi aN$, wherein N is the rotational speed in rpm and a is the diameter of the saw). Since the saw has 60 teeth (N_t), this would correspond to a tooth passing frequency ($NN_t/60$) of ~ 90 to ~ 225 Hz, i.e. the excitation frequencies would generally be limited to this range. The magnitude of the FRFs thus shown in Fig. 3 are plotted with respect to the excitation frequencies.

It is amply evident from the FRFs that the response of the guided saw is dynamically stiffer than the saw that is not. Like the case of the free vibration response, the dynamic stiffening is likely due to the stiffness of the fluid, with the damping, mass, and viscous shear of the fluid not playing a very significant role. Though the response of the guided saw is dynamically stiffer with smaller peak magnitudes than the one that is not guided, there are regimes of excitation frequencies for which the guided saw is more flexible than the unguided one. FRF characteristics in

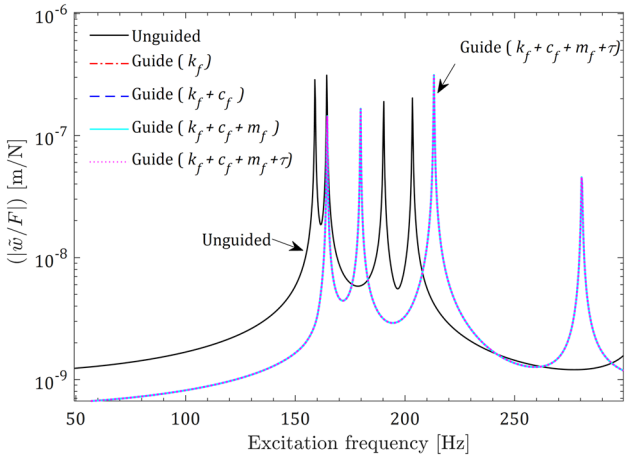

Fig. 3 Comparison of FRF characteristics for an oil-lubricated guided saw with a saw without a guide

Fig. 3 provide a global picture and help instruct selection of cutting speeds (rotational speeds) at which the response is low. Such analysis is new and useful.

Stability Characteristics for Differently Sized and Lubricated Guides

Stability of differently lubricated guided saws being influenced by a change in the size of a single-guide pad pair is

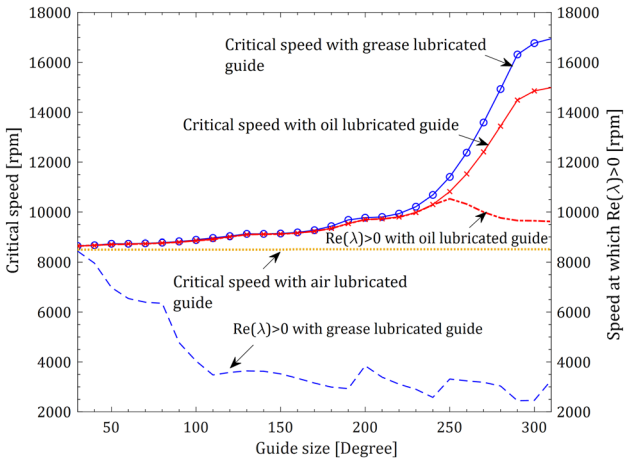

Fig. 4 Influence of changing the size of a single-guide pad pair on the stability of the saw

characterized in Fig. 4. The guide pad pair is assumed to start at $\gamma_1 = 22^0$, and its size is ranged from 30^0 up to 310^0 in increments of 10^0 in the counterclockwise direction. The limits on the size of the guide are chosen such that the guide does not interfere with the bar being cut. Since the individual influence of stiffness, damping, mass, and viscous shear was already characterized in the earlier sub-section, analysis herein is presented for fluids with all their mass, stiffness, damping, and shear stress influencing properties. Frequency–speed characteristics for differently lubricated guides follow the same trend as shown in Fig. 2 for the case of the oil-lubricated guides. As such, results shown in Fig. 4 are limited to the speed instants at which the system first becomes critical and at speed instants at which the real part of the eigenvalue becomes positive—suggesting growth in the free-vibration response that will also destabilize the system. These results are for the case of the gap between the saw and guide being 0.15 mm for all configurations.

As is evident from Fig. 4, for the case of the air-lubricated guide pads, since the stiffness of air is relatively low, critical speeds do not change with increasing guide sizes. However, since stiffness increases with the size of the guide, and since critical speeds increase with an in increase in stiffness, critical speeds for oil-lubricated and grease-lubricated guides are observed to increase. Since the real part for air-lubricated guides are always negative owing to internal damping in the system, it is not shown in Fig. 4. For the case of oil-lubricated guides, the critical speed and the speed at which the real part becomes positive appear to increase monotonically for guide sizes up to 250^0, beyond which the stability is limited by the real part of the eigenvalue and not the critical speed. For grease-lubricated guides larger than 30^0, the real part of the eigenvalue becomes positive before the critical speed is reached. The real part limiting stability is due to the viscous shear induced on the saw on account of the fluid's viscosity. Since the shear stress induced in the saw is proportional to the size of the guide pad, larger grease- and oil-lubricated guides tend to destabilize the saw before the onset of critical speeds.

Since the stability of air-lubricated guides does not change with guide size, and even though larger oil- and grease-lubricated guides destabilize the saw before onset of critical speeds, since the cutting speed regime of interest is significantly low, small and/or large oil-and grease-lubricated guides may indeed offer viable modes to stabilize circular sawing processes. As such, forced response is characterized for the representative case of grease-lubricated guides of different sizes in Fig. 5. The FRFs in Fig. 5 are shown for three representative guide sizes: one small and two larger ones.

As is evident from Fig. 5, for larger guide sizes, since the stiffness increases with the size of the guide, there is significant dynamic stiffening and correspondingly a significant shift in the natural frequencies. In the rotational speed/excitation frequency range of interest, an increase in the size of the guide pair from 30° to 150° results in the first mode shifting in frequency by ~ 16%. A further increase in the size of the guide to 230° shifts the first natural frequency by ~ 80%. Large guide sizes also result in the magnitude of the response reducing by an order and more. Similar behaviour is observed for the case of oil-lubricated guides.

Interestingly, the results in Fig. 5 suggest that cutting at the speed regimes of interest with large grease-lubricated guides results in low levels of forced vibration response when compared to cutting with unguided saws. On the other hand, results in Fig. 4 suggest that large grease-lubricated guides, due to the additional viscous shear stresses they induce in the saw, reduce the speed at which instability occurs first when compared to cutting with unguided or even air-lubricated and guided saws. Such analysis (as shown in

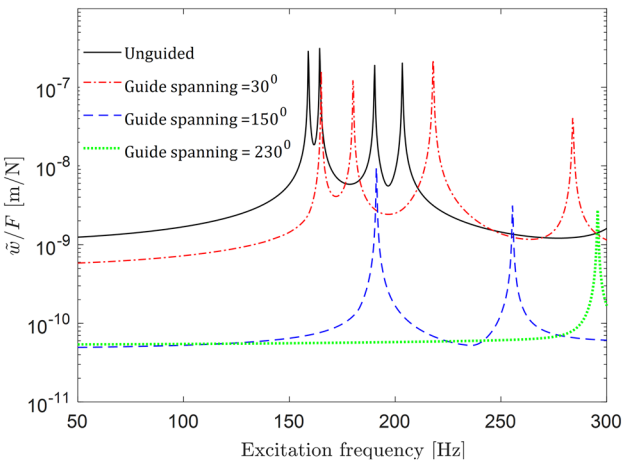

Fig. 5 Influence of changing size of the guide on the forced response characteristics for grease-lubricated guides

Figs. 4 and 5) is new and useful, since it can instruct on the appropriate selection of fluid media and the size of the guide that improve the critical speed and reduce the forced vibration response at cutting speed regimes of interest.

Stability Characteristics with Different Clearances Between the Saw and Differently Lubricated Guides

Stability for a single lubricated guide pair placed between $\gamma_1 = 22^0$ and $\gamma_2 = 52^0$ and with changing clearances between the saw and the guide is characterized in Fig. 6. For the gap ranging from 0.15 mm and up to 1 mm, with increments of 10 μm, the figure shows speed instants at which the system first becomes critical as well as speed instants at which the real part of the eigenvalue becomes positive. Results are shown for air-, oil-, and grease-lubricated guides, and in all cases, the fluid is modelled as a distributed mass, stiffness, and damping system with viscous shear.

As is evident from Fig. 6, stability of air-lubricated guides is unaffected by the clearances between the saw and the guide. As in the case of changing size of the guide, in this case too, internal damping in the saw keeps the real part of the eigenvalue always negative for air-lubricated guides, and hence that is not shown in Fig. 6. For the case of oil- and grease-lubricated guides, an increase in the clearance marginally reduces the first critical speed of the saw. This reduction is due to the stiffness of the fluid reducing with an increase in the clearance. Interestingly, for the oil- and the grease-lubricated guides, there are clearances at which there is a step change in the speed instants at which the real part of the eigenvalue becomes positive. Beyond the clearances at which these step changes occur, the speed instants at which the real part of the eigenvalue become positive are observed to reduce with increasing clearances. These changes are thought to occur due to the complex interactions between the shear intensity and the stiffness of the fluid changing with clearances. Unlike the influence of changing guide size for a fixed clearance, in the present case, stability is limited by the onset of the first critical speed, and not by the real part of the eigenvalues becoming positive at speed instances before critical.

Results in Fig. 6 suggest that for the size of the guide under consideration, since the critical speed reduces by < 1% for the clearance changing between 0.15 mm and up to 1 mm, larger clearances may not be disadvantageous. However, since our cutting speeds of interest are lower than the critical speed, guide placement relative to the saw must be done with due consideration to the forced vibration response changing with clearances. That analysis is shown in Fig. 7 for the representative case of grease-lubricated guides. Since the dynamics for air-lubricated guides remain relatively unaffected by changing clearances, and since the dynamics of oil-lubricated guides are like those of grease-lubricated guides, those results are not shown in Fig. 7. FRFs are shown for three representative levels of clearances.

As is evident from Fig. 7, the response with smaller clearances is dynamically stiffer than when the clearances are larger, and this is also due to stiffness being inversely proportional to the clearances. Importantly, even with larger clearances, the response is still dynamically stiffer than a saw that is not guided. However, there remain regimes of excitation frequencies for which the guided saw is more flexible than the unguided one. Since the results in Figs. 6 and 7 are only for a small size of the guide, and though for this size the results suggest that any clearance is acceptable, results in Fig. 5 already show that larger guides are better from

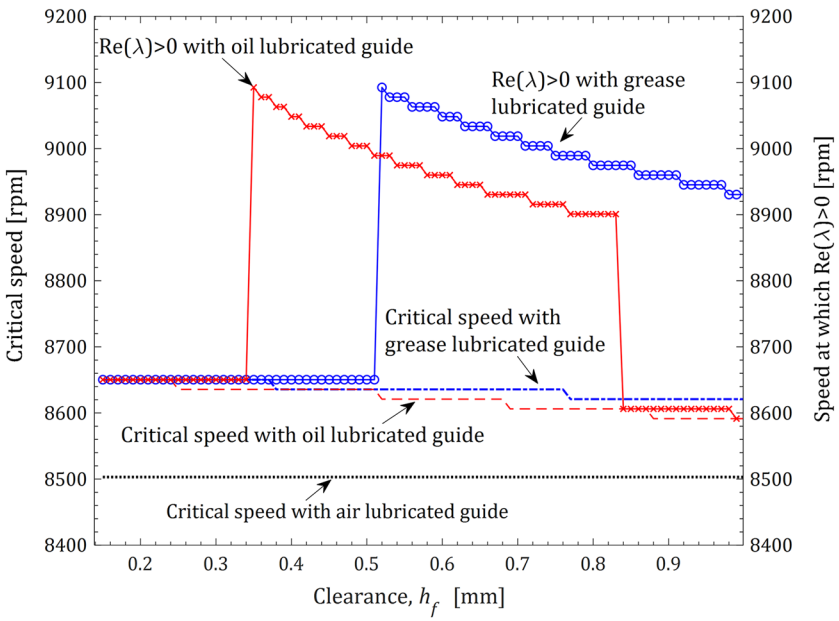

Fig. 6 Influence of changing clearances between the saw and differently lubricated guides

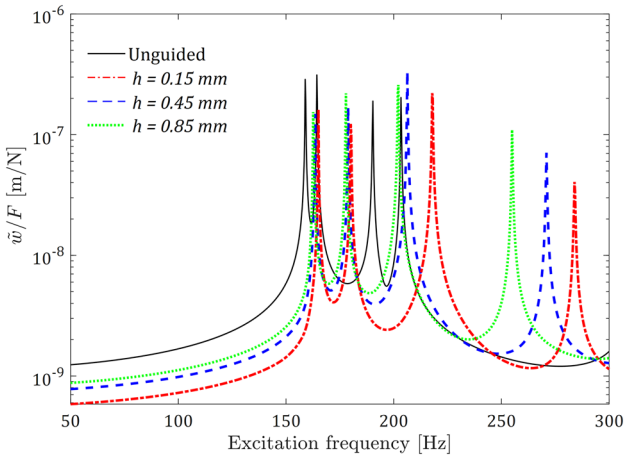

Fig. 7 Forced response characteristics changing with clearances (h_f) between the saw and grease-lubricated guides

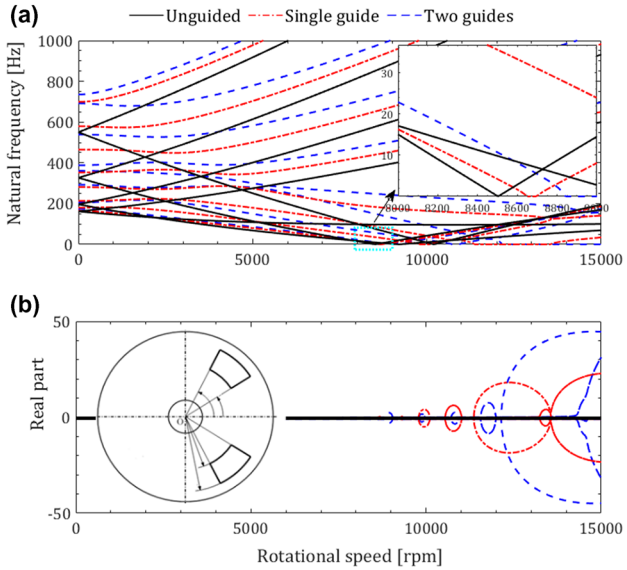

Fig. 8 Comparison of speed characteristics for a saw with two oil-lubricated guides with that of a single oil-lubricated guided saw and a saw without a guide. **a** Frequency–speed characteristics. **b** Real part of the eigenvalue changing with speed

the forced response perspective, as such, while deciding on how near the saw to place the guides, it is also important to factor the guide size as well as the fluid media to be used. Such analysis is facilitated by our models making them furthermore useful.

Multiple Oil-Lubricated Guides

This section discusses the stability and the forced response characteristics of a saw constrained laterally by two guide pad pairs placed symmetrically across the cutting region. A schematic of this configuration is shown within the inset in Fig. 8. The first guide pad pair is placed between $\gamma_1 = 22^0$ and $\gamma_2 = 52^0$, and the second is placed between $\gamma_1 = 308^0$ and $\gamma_2 = 338^0$—making the size of each guide pad pair fixed to be 30^0. For analysis herein, the clearance between the saw and the guides was fixed to be 0.15 mm. Only the representative case of oil-lubricated guides is considered herein with the fluid modelled as being a distributed mass, stiffness, and damping system with viscous shear. As for the single-guide case, herein too, for the forced excitation case, the response was evaluated at the outer edge of the middle of the sector in contact with the workpiece, i.e. at $\gamma = 0^o$. The resulting frequency–speed characteristics are shown in Fig. 8, and the forced vibration characteristics of this configuration are shown in Fig. 9. Results for the two-guide pad pairs are contrasted with a single-guide pad pair with the same size and clearance, and for the same oil (fluid) properties as discussed in the earlier sub-section. In both cases, response is contrasted with a saw that is not guided.

As is evident from Fig. 8, the first critical speed for the two-guide case is higher than the single-guide case. Also noteworthy is that this improvement in the critical speed for two guides that effectively spans 60° is almost the same as that of a single guide that spans 100° (see Fig. 4)—suggesting that the use of distributed multiple guides may prove more useful to stabilize circular sawing processes than the use of large single guides. Interestingly, even with the two-guide case, the mode to first become critical is the 0.1 mode, i.e. the same mode as in the single-guide case. Though the two-guide case results in an improved critical speed, and even though the frequency–speed characteristics for this case are different from the single-guide and the unguided case, in the super-critical regimes, the two-guide case results in

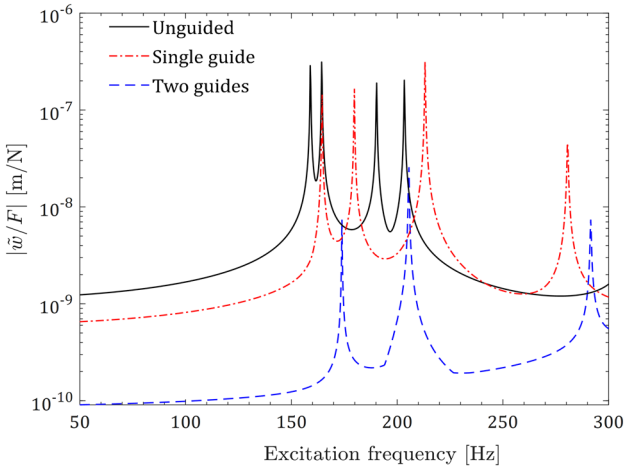

Fig. 9 Comparative analysis for forced response characteristics for a two-guide case with that of a single-guide case and for a saw that is not guided

wider regions of instabilities, with higher rates of growth—see Fig. 8b. However, since the metal cutting speed regimes of interest are significantly lower than the critical, and since the critical speeds improve with two oil-lubricated guides, behaviour in the super-critical regimes are not very consequential from the use case scenario of interest herein.

As is evident from the forced response characteristics shown in Fig. 9, the FRF for the two-guide case is significantly dynamically stiffer than the single-guide case. The first natural frequency increases by ~ 10% over the unguided case as compared to an increase by ~ 4% for the single-guide case. The magnitude of the response is also more than an order of magnitude lesser for the two-guide case as compared to the unguided and/or the single-guide case. This dynamic stiffening for two guides effectively spanning 60^0 is almost the same as that of a single guide that spans 150^0 (see Fig. 5). This confirms that two oil-lubricated guides outperform large single guides in terms of improving the critical speed and dynamically stiffening the system.

Though Figs. 8 and 9 present results for only oil-lubricated multiple guides for a fixed size of the guides and for a fixed clearance between the saw and the guides, and even though analysis with different lubricating fluids, changing size of multiple guides, and with changing clearances was carried out, since those findings follow the general trends reported already for the single-guide pad pair case, those results are not presented here for the sake of brevity. Since the proposed model is generalized enough to facilitate analysis with even more number of guide pad pairs as necessitated by the application of interest, the models are furthermore useful.

Conclusions

Metal cutting circular saws are guided and lubricated. Since the lubricating fluid has mass, damping, and stiffness properties, and since the fluid induces viscous shear stresses on the saw, it contributes to the in-plane stress of the saw. Since guides are distributed and can number more than one, the fluid can be anything, and the clearance between the saw and the guide can be variable, characterizing the role of lubricated and distributed guides on the dynamics and stability of metal cutting circular saws was the main aim of this paper. Models proposed to facilitate such analysis are our new and modest contribution to the state of the art.

From our systematic model-based investigations, we conclude that:

1. the stiffness of the fluid media plays a more significant role than its mass, damping, and/or viscosity.
2. the grease- and oil-lubricated guides improve critical speeds more than air-lubricated guides.
3. there is no significant difference in the dynamics and stability of saws with guides that are air lubricated and saws that are not guided.
4. for larger oil- and grease-lubricated guides, the stability of the saw is governed by growth in the response and not by critical speeds, and the forced response of the oil- and grease-lubricated and guided saws is at least an order of magnitude dynamically stiffer than air-lubricated and guided saws.
5. smaller clearances between the saw and the guide are better from the stability and dynamic stiffening perspective.
6. two lubricated guides are dynamically stiffer than one and they result in improved critical speeds when compared to a single guide and an unguided saw.

Though there is a need for experimental validation of our model-based observations, and though that can form part of future studies, since our treatment of lubricated guides is realistic, our findings can still instruct the design of stable guided metal sawing processes in industries. For example, for those wanting to cut metal at low speeds, since critical speeds would not limit cutting, the focus could instead be to add two or more small grease-lubricated guides that would reduce the forced vibration response characteristics, and hence improve the cutting behaviour as well as the life of the saw. For those wanting to cut at higher speeds, to improve productivity and yet avoid critical speeds, the focus could be instead on using larger oil-lubricated guides. In all cases, guides should be placed circumferentially near the cutting zone and with small clearances between the saw and the guide.

Acknowledgements This research was supported by the Government of India's Science and Engineering Research Board's Early Career Research Award—SERB/ECR/2016/000619. The authors acknowledge Mr. Praveen Kumar and Dr. Shakti Gupta for their useful and insightful technical inputs.

Declarations

Conflict of interest On behalf of all authors, the corresponding author states that there is no conflict of interest.

References

1. Szymani R, Mote CD (1977) Principal developments in thin circular saw vibration and control research. Holz als Roh-und Werkstoff 35(6):219–225. https://doi.org/10.1007/BF02608337
2. Schajer GS (1986) Why are guided circular saws more stable than unguided saws? Holz als Roh-und Werkstoff 44:465–469. https://doi.org/10.1007/BF02608068

3. Lehmann BF, Hutton SG (1988) Self-excitation in guided circular saws. J Vib Acoust Stress Reliab 110:338–344. https://doi.org/10.1115/1.3269522
4. Iwan WD, Moeller TL (1976) The stability of a spinning elastic disk with a transverse load system. J Appl Mech 4:485–490. https://doi.org/10.1115/1.3423896
5. Benson RC, Bogy DB (1978) Deflection of a very flexible spinning disk due to a stationary transverse load. J Appl Mech 45:636–642. https://doi.org/10.1115/1.3424374
6. Hutton SG, Chonan S, Lehmann BF (1987) Dynamic response of a guided circular saw. J Sound Vib 112:527–539. https://doi.org/10.1016/S0022-460X(87)80116-5
7. Chen JS, Bogy DB (1992) Effects of load parameters on the natural frequencies and stability of a flexible spinning disk with a stationary load system. J Appl Mech 59:S230–S235. https://doi.org/10.1115/1.2899494
8. Tseng JG, Wickert JA (1997) Nonconservative stability of a friction loaded disk. In: International design engineering technical conferences and computers and information in engineering conference, vol 80432, p V01DT20A015. https://doi.org/10.1115/DETC97/VIB-4087
9. Norouzi H, Younesian D (2022) Analytical modeling of transverse vibrations and acoustic pressure mitigation for rotating annular disks. Math Probl Eng. https://doi.org/10.1155/2022/3722410
10. Mote CD (1977) Moving-load stability of a circular plate on a floating central collar. J Acoust Soc Am 61:439–447. https://doi.org/10.1121/1.381284
11. Shen IY (1993) Response of a stationary, damped, circular plate under a rotating slider bearing system. J Vib Acoust 115:65–69. https://doi.org/10.1115/1.2930316
12. Chan SN, Mottershead JE, Cartmell MP (1994) Parametric resonances at subcritical speeds in discs with rotating frictional loads. Proc Inst Mech Eng C J Mech Eng Sci 208:417–425. https://doi.org/10.1243/PIME_PROC_1994_208_147_02
13. Mottershead JE, Ouyang H, Cartmell MP, Friswell MI (1997) Parametric resonances in an annular disc, with a rotating system of distributed mass and elasticity; and the effects of friction and damping. Proc R Soc Lond Ser A Math Phys Eng Sci 453:1–19. https://doi.org/10.1098/rspa.1997.0001
14. Ouyang H, Mottershead JE (2001) Optimal suppression of parametric vibration in discs under rotating frictional loads. Proc Inst Mech Eng C J Mech Eng Sci 215:65–75. https://doi.org/10.1243/0954406011520526
15. Younesian D, Aleghafourian MH, Esmailzadeh E (2015) Vibration analysis of circular annular plates subjected to peripheral rotating transverse loads. J Vib Control 21(7):1443–1455. https://doi.org/10.1177/1077546313499178
16. Hutton SG (1991) The dynamics of circular saw blades. Holz als Roh-und Werkstoff 49:105–110. https://doi.org/10.1007/BF02614349
17. Khorasany RM, Mohammadpanah A, Hutton SG (2012) Vibration characteristics of guided circular saws: experimental and numerical analyses. J Vib Acoust. https://doi.org/10.1115/1.4006650
18. Mohammadpanah A, Hutton SG (2015) Flutter instability speeds of guided splined disks: an experimental and analytical investigation. Shock Vib. https://doi.org/10.1115/1.4006650
19. Khorasany RM, Hutton SG (2007) A stability analysis of constrained rotating disks with different boundary conditions. Turbo Expo Power Land Sea Air 47942:335–342. https://doi.org/10.1115/GT2007-27341
20. Singhania S, Kumar P, Gupta SK, Law M (2019) Influence of guides on critical speeds of circular saws. In: Advances in computational methods in manufacturing. Springer, pp 519–530. https://doi.org/10.1007/978-981-32-9072-3_45
21. Ono K, Chen JS, Bogy DB (1991) Stability analysis for the head-disk interface in a flexible disk drive. ASME J Appl Mech 58:1005–1014. https://doi.org/10.1115/1.2897675
22. Chan SN, Mottershead JE, Cartmell MP (1995) Instabilities at subcritical speeds in discs with rotating frictional follower loads. ASME Trans J Vib Acoust 117:240–242. https://doi.org/10.1115/1.2873936
23. Ouyang H, Chan SN, Mottershead JE, Friswell MI, Cartmell MP (1995) Parametric vibrations in discs: point-wise and distributed loads, including rotating friction. In: International design engineering technical conferences and computers and information in engineering conference, vol 17186, pp 1125–1133. https://doi.org/10.1115/DETC1995-0359
24. Yang F, Pei YC (2022) A thermal stress stiffening method for vibration suppression of rotating flexible disk with mass-spring-damper system loaded. Int J Mech Sci 213:106860. https://doi.org/10.1016/j.ijmecsci.2021.106860
25. Hosaka H, Crandall SH (1992) Self-excited vibrations of a flexible disk rotating on an air film above a flat surface. Advances in dynamic systems and stability. Acta Mech. https://doi.org/10.1007/978-3-7091-9223-8_9
26. Huang FY, Mote CD (1995) On the instability mechanisms of a disk rotating close to a rigid surface. J Appl Mech 62:764–771. https://doi.org/10.1115/1.2897012
27. Mote CD, Nieh LT (1973) On the foundation of circular-saw stability theory. Wood Fiber Sci 5:160–169
28. Mohammadpanah A, Hutton SG (2017) Theoretical and experimental verification of dynamic behaviour of a guided spline arbor circular saw. Shock Vib. https://doi.org/10.1155/2017/6213791
29. Mohammadpanah A, Hutton SG (2021) Dynamic response of guided spline circular saws vs. collared circular saws, subjected to external loads. Wood Mater Sci Eng 16(3):166–169. https://doi.org/10.1080/17480272.2019.1644371
30. Takkar S, Gupta K, Tiwari V, Singh SP (2019) Dynamics of rotating composite disc. J Vib Eng Technol 7:629–637. https://doi.org/10.1007/s42417-019-00155-8
31. Hagedorn P, DasGupta A (2007) Vibrations and waves in continuous mechanical systems. Wiley, New York
32. Mickens RE (2010) Truly nonlinear oscillations: harmonic balance, parameter expansions, iteration, and averaging methods. World Scientific, Singapore
33. Kumar P (2020) Influence of guide induced friction on the dynamics and stability of guided circular sawing, M.Tech. thesis, Indian Institute of Technology Kanpur
34. Singh A (2021) Regenerative instabilities of metal cutting circular saws with lubricated and distributed guides, M.Tech. thesis, Indian Institute of Technology Kanpur
35. CSAW 4.0 Computer software for optimizing circular saw design, Wood Mach. Institute, Berkeley, CA USA, 2007
36. SKF lubricants (2018). https://www.skf.com/binaries/pub12/Images/0901d196802103bc13238EN_GreaseSelectionChart_tcm_12-99598.pdf. Accessed July 2021
37. Zhuo R, Deng Z, Chen B, Guoyue L, Shenghao B (2021) Overview on development of acoustic emission monitoring technology in sawing. Int J Adv Manuf Technol 116:1411–1427. https://doi.org/10.1007/s00170-021-07559-5